International Journal of Mechanical Engineering Research
And Development (IJMERD), ISSN 2248 – 9347(Print)
ISSN 2248 – 9355(Online), Volume 3, Number 1
Jan - March (2013), pp.11- 27
© PRJ Publication, http://www.prjpublication.com/IJMERD.asp

IJMERD

© PRJ PUBLICATION

COMPUTATIONAL BUCKLING OF A THREE-LOBED CROSECTION CYLINDRICAL SHELL WITH VARIABLE THICKNESS UNDER COMBINED COMPRESSION AND BENDING LOADS

MOUSA KHALIFA AHMED
Department of mathematics, Faculty of science at Qena,
South valley university, Egypt
E-mail: mousa@japan.com

ABSTRACT

The objective of this paper is to study the elastic buckling characteristics of an axially loaded cylindrical shell of a three lobed cross section of variable thickness subjected to combined compression and bending loads based on the thin-shell theory and using the computational transfer matrix method. Modal displacements of the shell can be described by trigonometric functions and Fourier's approach is used to separate the variables. The governing equations of the shell are reduced to eight first-order differential equations with variable coefficients in the circumferential coordinate, and by using the transfer matrix of the shell, these equations can be written in a matrix differential equation. The transfer matrix is derived from the non-linear differential equations of the cylindrical shells by introducing the trigonometric function in the longitudinal direction and applying a numerical integration in the circumferential direction. The computational transfer matrix method is used to get the critical buckling loads and the buckling deformations for symmetrical and antisymmetrical buckling-modes. Computed results indicate the sensitivity of the critical loads and corresponding buckling modes to the thickness variation of cross-section and the radius variation at lobed corners of the shell.

KEYWORDS: Buckling characteristic, Stability, Transfer matrix method, Non-circular cylindrical shell, Non-uniform axial loads, and Variable thickness.

1. INTRODUCTION

The use of cylindrical shells which have non-circular profiles is common in many fields, such as aerospace, mechanical, civil and marine engineering structures. The displacements buckling modes of thin elastic shells essentially depend on some determining functions such as the radius of the curvature of the neutral surface, the shell thickness, the shape of the shell edges, etc. In simple cases when these functions are constant, the buckling modes occupy the entire shell surface. If the determining functions vary from point to point of the neutral surface then localization of the displacements buckling modes lies near the weakest lines on the shell surface, and this kind of problems is too difficult because the radius of its curvature varies with the circumferential coordinate, closed-form or analytic solutions cannot be obtained, in general, for this class of shells, numerical or approximate techniques are necessary for their analysis. Buckling has become more of a problem in recent years since the use of high strength material requires less material for load support-structures and components have become generally more

slender and buckle-prone. Many researchers have considerable interest in the study of stability problems of circular cylindrical shells under uniform axial loads with constant thickness and numerous investigations have been devoted to this. e.g[1-9]. Other related references may be found in the well-known work of Love [10] in 1944, Flügge [11] in 1973 and Tovstik [12] in 1995. In contrast, the buckling behaviour under applied non-uniform axial loads has received much less attention, but some of treatments are found in [13-17], and Song [18] in 2002 provided a review of research and trends in the area of stability of un-stiffened circular cylindrical shells under non-uniform axial loads. Recently, with the advent of the high speed digital computer, the buckling study of shells directed to ones with complex geometry, such as the variability of radius of curvature and thickness. Using the modified Donell-type stability equations of cylindrical shells with applying Galerkin's method, the stability of cylindrical shells with variable thickness under dynamic external pressure is studied by Abdullah and Erdem [19] in 2002. Eliseeva et al. and Filippov et al. [20-21] in 2003 and 2005 presented the vibration and buckling of cylindrical shells of variable thickness with slanted and curvelinear edges, respectively, using the asymptotic and finite element methods. As analytical solutions for axisymmetric transverse vibration of cylindrical shells with thickness varying in power form due to forces acting in the transverse direction are derived for the first time by Duan and Koh [22] in 2008. Sambandam et al.[23] in 2003 studied the buckling characteristics of cross-ply elliptical cylindrical shells under uniform axial loads based on the higher-order theory and found that an increase in the value of radius to thickness ratio the critical load decreases. Using the generalized beam theory, the influence of member length on the critical loads of elliptical cylindrical shells under uniform compression is studied by Silvestre [24] in 2008. By the use of the transfer matrix method and based on the theories of thin-shell and Flügge's shell, Khalifa [25-27] in 2010 and 2011 studied the vibration and buckling behaviour of non-circular cylindrical shells. A treatise on the use of the transfer matrix approach for mechanical science problems is presented by Tesar and Fillo [28] in 1988. However, the problem of stability of the shell-type structures treated here which are composed of circular cylindrical panels and flat plates with circumferential variable thickness under non-uniform loads does not appear to have been dealt with in the literature. The aim of this paper is to present the buckling behaviour of an isotropic cylindrical shell with a three lobed cross section of circumferentially varying thickness, subjected to non-uniformly compressive loads, using the transfer matrix method and modeled on the thin-shell theory. The proposed method is applied to symmetrical and antisymmetrial buckling-modes. The critical buckling loads and corresponding buckling deformations of the shell are presented. The influences of the thickness variation and radius variation on the buckling characteristics are examined. The results are cited in tabular and graphical forms.

2. THEORY AND FORMULATION OF THE PROBLEM

It has been mentioned in introduction section that the problem structure is modeled by thin-shell theory. In order to have a better representation, the shell geometry and governing equations are modeled as separate parts. The formulation of these parts is presented below.

2.1. GEOMETRICAL FORMULATION

We consider an isotropic, elastic, cylindrical shell of a three-lobed cross-section profile expressed by the equation $r = a\, f(\theta)$, where r is the varied radius along the cross-section mid-line, a is the reference radius of curvature, chosen to be the radius of a circle having the same circumference as the three-lobed profile, and $f(\theta)$ is a prescribed function of θ and can be described as:

$$f(\theta)=a_1\begin{Bmatrix} 2(1-\zeta)\cos\theta+\sqrt{\zeta^2-4(1-\zeta)^2\sin^2\theta}, & 0\le\theta\le\theta_1 \\ \cos ec(\theta+30^0), \quad \rho=0, & \theta_1\le\theta\le 120^0-\theta_1 \\ 2(1-\zeta)\cos(\theta-120^0)+\sqrt{\zeta^2-4(1-\zeta)^2\sin^2(\theta-120^0)}, & 120^0-\theta_1\le\theta\le 120^0+\theta_1 \\ -\sec\theta, \quad \rho=0, & 120^0+\theta_1\le\theta\le 180^0 \end{Bmatrix}, \quad (1)$$

$$a_1=A_1/a, \quad \rho=a/R_1, \zeta=R_1/A_1, \quad \theta_1=\tan^{-1}\left\{\sqrt{3}/(4/\zeta-\sqrt{3})\right\}.$$

L_1 and L_2 are the axial and circumferential lengths of the middle surface of the shell, and the thickness $H(\theta)$ varying continuously in the circumferential direction. The cylindrical coordinates (x, s, z) are taken to define the position of a point on the middle surface of the shell, as shown in Figure (1.1) and Figure (1.2) shows the three-lobed cross-section profile of the middle surface, with the apothem denoted by A_1, and the radius of curvature at the lobed corners by R_1. While u, v and w are the deflection displacements of the middle surface of the shell in the longitudinal, circumferential and transverse directions, respectively. We suppose that the shell thickness H at any point along the circumference is small and depends on the coordinate θ and takes the following form:

$$H(\theta)=h_0\,\varphi(\theta) \quad (2)$$

where h_0 is a small parameter, chosen to be the average thickness of the shell over the length L_2. For the cylindrical shell which cross-section is obtained by the cutaway the circle of the radius r_0 from the circle of the radius R_0 (see Figure (1.3) function $\varphi(\theta)$ have the form: $\varphi(\theta)=1+\delta(1-\cos\theta)$, where δ is the amplitude of thickness variation, $\delta=d/h_0$, and d is the distance between the circles centers. In general case $h_0=H(\theta=0)$ is the minimum value of $\varphi(\theta)$ while $h_m=H(\theta=\pi)$ is the maximum value of $\varphi(\theta)$, and in case of $d=0$ the shell has constant thickness h_0. The dependence of the shell thickness ratio $\eta=h_m/h_0$ on δ has the form $\eta=1+2\delta$.

2.2. GOVERNING EQUATIONS

For a general circular cylindrical shell subjected to a non-uniform circumferentially compressive load $p(\theta)$, the static equilibrium equations of forces, based on the Goldenveizer-Novozhilov theory [29-30] in 1961 and 1964 can be shown to be of the forms:

$$\begin{aligned} &N_x'+N_{sx}^{\bullet}-P(\theta)u''=0, \quad && N_{xs}'+N_s^{\bullet}+Q_s/R-P(\theta)v''=0, \\ &Q_x'+Q_s^{\bullet}-N_s/R-P(\theta)w''=0, \quad && M_x'+M_{sx}^{\bullet}-Q_x=0, \\ &M_{xs}'+M_s^{\bullet}-Q_s=0, \quad && S_s-Q_s-M_{sx}'=0, \quad N_{xs}-N_{sx}-M_{sx}/R=0, \end{aligned} \quad (3)$$

where N_x, N_s and Q_x, Q_s are the normal and transverse shearing forces in the x and s directions, respectively, N_{sx} and N_{xs} are the in-plane shearing forces, M_x, M_s and M_{xs}, M_{sx} are the bending moment and the twisting moment, respectively, S_s is the equivalent (Kelvin-Kirchoff) shearing force, R is the radius of curvature of the middle surface, $'\equiv\partial/\partial x$, and

$^{\bullet} \equiv \partial / \partial s$. We assume that the shell is loaded along the circumferential coordinate by non-uniform axial loads $p(\theta)$ which vary with θ, where the compressive load does not reach its critical value at which the shell loses stability. Generally, the form of the load may be expressed as:

$$p(\theta) = p_0\, g(\theta) \tag{4}$$

where $g(\theta)$ is a given function of θ and p_0 is a constant. We consider the shell is loaded by non-uniform loads, combined compression and bending loads, (per unit length) given by [13] in 1932 as:

$$p(\theta) = p_0(1+2\cos\theta), \qquad g(\theta) = 1+2\cos\theta \tag{5}$$

and the sketch depicting this load is given in Figure (1.4). The applied specific load in this form establishes two zones on the shell surface: one is the compressive zone, Q_1, for $(0<\theta<2\pi/3)$ where the buckling load factor is a maximum and the thickness is a minimum and the other is the tensile zone, Q_2, for $(2\pi/3<\theta<\pi)$ where the buckling load factor is a minimum and the thickness is a maximum, as shown in this figure. Note that $p(\theta) = p_0$ in the case of applied compression loads. Hereby, we deduce the following ratio of critical loads:

$$\mu = \frac{p_C \ for \ compression \ loads}{p_C \ for \ combined \ loads}, \tag{6}$$

p_C Is the lowest value of applied compressive loads and named by the critical load.
The relations between strains and deflections for the cylindrical shells used here are taken from [31] in 1973 as follows:

$$\begin{aligned} &\varepsilon_x = u', \qquad \varepsilon_s = \upsilon^{\bullet} + w/R, \qquad \gamma_{xs} = \upsilon' + u^{\bullet}, \qquad \gamma_{xz} = w' + \psi_x = 0, \\ &\gamma_{sz} = w^{\bullet} + \psi_s - \upsilon/R = 0, \quad k_x = \psi_x', \quad k_s = \psi_s^{\bullet} + (\upsilon^{\bullet} + w/R)/R, \quad k_{sx} = \psi_s', \quad k_{xs} = \psi_x^{\bullet} + \upsilon'/R \end{aligned} \tag{7}$$

where ε_x and ε_s are the normal strains of the middle surface of the shell, γ_{xs}, γ_{xz} and γ_{sz} are the shear strains, and the quantities k_x, k_s, k_{sx} and k_{xs} representing the change of curvature and the twist of the middle surface, ψ_x is the bending slope, and ψ_s is the angular rotation. The components of force and moment resultants in terms of Eq. (7) are given as:

$$\begin{aligned} &N_x = D(\varepsilon_x + \nu\varepsilon_s), \quad N_s = D(\varepsilon_s + \nu\varepsilon_x), \quad N_{xs} = D(1-\nu)\gamma_{xs}/2, \\ &M_x = K(k_x + \nu k_s), \quad M_s = K(k_s + \nu k_x), \quad M_{sx} = k(1-\nu)k_{sx}. \end{aligned} \tag{8}$$

From Eqs. (3) to (8), with eliminating the variables Q_x, Q_s, N_x, N_{xs}, M_x, M_{xs} and M_{sx} which are not differentiated with respect to s, the system of the partial differential equations for the state variables $u, \upsilon, w, \psi_s, M_s, S_s, N_s$ and N_{sx} of the shell are obtained as follows:

$$\begin{aligned} &u^{\bullet} = 2/(D(1-\nu))N_{sx} + (H^2/6R)\psi_s' - \upsilon', \qquad \upsilon^{\bullet} = N_s/D - w/R - \nu u', \qquad w^{\bullet} = \upsilon/r - \psi_s, \\ &\psi_s^{\bullet} = M_s/K + \nu\psi_x' - N_s/RD - (\nu/R)u', \qquad M_s^{\bullet} = S_s - 2K(1-\nu)\psi_s'', \\ &S_s^{\bullet} = N_s/R - \nu M_s'' + K(1-\nu^2)w''' + P(\theta)w'', \qquad N_s^{\bullet} = P(\theta)\upsilon'' - S_s/R - N_{sx}' \\ &N_{sx}^{\bullet} = D(1-\nu^2)u'' + P(\theta)u'' - \nu N_s'. \end{aligned} \tag{9}$$

The quantities D and K, respectively, are the extensional and flexural rigidities expressed in terms of the Young's modulus E, Poisson's ratio ν and the wall thickness $H(\theta)$ as the form: $D = EH/(1-\nu^2)$ and $K = EH^3/12(1-\nu^2)$, and on considering the variable thickness of the shell, using Eq. (1), they take the form:

$$D = (Eh_0/(1-\nu^2))\varphi(\theta) = D_0\,\varphi(\theta), \tag{10}$$

$$K = (E(h_0)^3/(1-\nu^2))\varphi^3(\theta) = K_0\,\varphi^3(\theta) \tag{11}$$

Where D_0 and K_0 are the reference extensional and flexural rigidities of the shell, chosen to be the averages on the middle surface of the shell over the length L_2.

For a simply supported shell, the solution of the system of Eqs (9) is sought as follows:

$$\begin{aligned}
&u(x,s) = \overline{U}(s)\cos\beta x, \quad (v(x,s), w(x,s)) = (\overline{V}(s), \overline{W}(s))\sin\beta x, \quad \psi_s(x,s) = \overline{\psi}_s(s)\sin\beta x,\\
&(N_x(x,s), N_s(x,s), Q_s(x,s), S_s(x,s)) = (\overline{N}_x(s), \overline{N}_s(s), \overline{Q}_s(s), \overline{S}_s(s))\sin\beta x,\\
&(N_{xs}(x,s), N_{sx}(x,s), Q_x(x,s)) = (\overline{N}_{xs}(s), \overline{N}_{sx}(s), \overline{Q}_x(s))\cos\beta x,\\
&(M_x(x,s), M_s(x,s)) = (\overline{M}_x(s), \overline{M}_s(s))\sin\beta x,\\
&(M_{xs}(x,s), M_{sx}(x,s)) = (\overline{M}_{xs}(s), \overline{M}_{sx}(s))\cos\beta x, \qquad \beta = m\pi/L_1, \qquad m = 1,2,...
\end{aligned} \tag{12}$$

Where m is the axial half wave number and the quantities $\overline{U}(s), \overline{V}(s), ...$ are the state variables and undetermined functions of s.

3. MATRIX FORM OF THE BASIC EQUATIONS

The differential equations as shown previously are modified to a suitable form and solved numerically. Hence, by substituting Eqs (12) into Eqs. (9), after appropriate algebraic operations and take relations (10) and (11) into account, the system of buckling equations of the shell can be written in non-linear ordinary differential equations referred to the variable s only are obtained, in the following matrix form:

$$a\frac{d}{ds}\begin{Bmatrix} \tilde{U}\\ \tilde{V}\\ \tilde{W}\\ \tilde{\psi}_s\\ \tilde{M}_s\\ \tilde{S}_s\\ \tilde{N}_s\\ \tilde{N}_{sx} \end{Bmatrix} = \begin{bmatrix} 0 & V_{12} & 0 & V_{14} & 0 & 0 & 0 & V_{18}\\ V_{21} & 0 & V_{23} & 0 & 0 & 0 & V_{27} & 0\\ 0 & V_{32} & 0 & V_{34} & 0 & 0 & 0 & 0\\ V_{41} & 0 & V_{43} & 0 & V_{45} & 0 & V_{47} & 0\\ 0 & 0 & 0 & V_{54} & 0 & V_{56} & 0 & 0\\ 0 & 0 & V_{63} & 0 & V_{65} & 0 & V_{67} & 0\\ 0 & V_{72} & 0 & 0 & 0 & V_{76} & 0 & V_{78}\\ V_{81} & 0 & 0 & 0 & 0 & 0 & V_{87} & 0 \end{bmatrix} \begin{Bmatrix} \tilde{U}\\ \tilde{V}\\ \tilde{W}\\ \tilde{\psi}_s\\ \tilde{M}_s\\ \tilde{S}_s\\ \tilde{N}_s\\ \tilde{N}_{sx} \end{Bmatrix}. \tag{13}$$

By using the state vector of fundamental unknowns $Z(s)$, system (13) can be written as:

$$(a\frac{d}{ds})\{Z(s)\} = [V(s)]\{Z(s)\} \tag{14}$$

$$\{Z(s)\}=\{\tilde{U},\tilde{V},\tilde{W},\tilde{\psi}_s,\tilde{M}_s,\tilde{S}_s,\tilde{N}_s,\tilde{N}_{sx}\}^T,$$

$$(\tilde{U},\tilde{V},\tilde{W})=k_0(\overline{U},\overline{V},\overline{W}),\quad \tilde{\psi}_s=(k_0/\beta)\overline{\psi}_s,\quad \tilde{M}_s=(1/\beta^2)\overline{M}_s,$$
$$(\tilde{S}_s,\tilde{N}_s,\tilde{N}_{sx})=(1/\beta^3)(\overline{S}_s,\overline{N}_s,\overline{N}_{sx}).$$

For the non-circular cylindrical shell which cross-section profile is obtained by function ($r=a\,f(\theta)$), the hypotenuse (ds) of a right triangle whose sides are infinitesimal distances along the surface coordinates of the shell takes the form:

$(ds)^2=(dr)^2+(r\,d\theta)^2$, then we have: $\dfrac{ds}{a}=\sqrt{(f(\theta))^2+(\dfrac{df(\theta)}{d\theta})^2}\;d\theta$ (15)

Using Eq. (15), the system of buckling equations (14) takes the form:

$$(\frac{d}{d\theta})\{Z(\theta)\}=\Psi(\theta)[V(\theta)]\{Z(\theta)\},\tag{16}$$

Where $\Psi(\theta)=\sqrt{(f(\theta))^2+(\dfrac{df(\theta)}{d\theta})^2}$, and the coefficients Matrix $[V(\theta)]$ are given as:

$V_{12}=-(m\pi/l)$, $V_{14}=(m\pi/l)^2(h^2/6)\varphi$, $V_{18}=(m\pi/l)^3(h^2/6(1-\nu)\varphi)$, $V_{21}=\nu(m\pi/l)$,
$V_{23}=-\rho$, $V_{27}=(m\pi/l)^3(h^2/12\varphi)$, $V_{32}=\rho$, $V_{34}=-(m\pi/l)$, $V_{41}=-\nu\rho$,
$V_{43}=-\nu(m\pi/l)^2$, $V_{45}=1/h\varphi^3$, $V_{46}=\rho h/12\varphi^2$, $V_{54}=2(1-\nu)h(m\pi/l)^2\varphi^2$,
$V_{56}=1$, $V_{63}=(1-\nu)(m\pi/l)\varphi/2-\overline{p}g/(m\pi/l)$,
$V_{65}=\nu(m\pi/l)$, $V_{67}=\rho(m\pi/l)$, $V_{72}=-\overline{p}g/(m\pi/l)$,
$V_{76}=-\rho$, $V_{78}=m\pi/l$, $V_{81}=\varphi(1-\nu^2)(12/h^2)/m\pi/l-\overline{p}g/(m\pi/l)$, (17)
$V_{87}=-\nu(m\pi/l)$ In terms of the following dimensionless shell parameters:

Curvature parameter $\rho=a/R$, buckling load factor $\overline{p}=p_0(a^2/K_0)$, $l=L_1/a$, and $h=h_0/a$.
The state vector $\{Z(\theta)\}$ of fundamental unknowns can be easily expressed as:

$$\{Z(\theta)\}=[Y(\theta)]\{Z(0)\}\tag{18}$$

By using the transfer matrix $[Y(\theta)]$ of the shell, and the substitution of the expression into Eq. (16) yields:

$$(d/d\theta)[Y(\theta)]=\Psi(\theta)[V(\theta)][Y(\theta)],\qquad [Y(0)]=[I].\tag{19}$$

The governing system of buckling (19) is too complicated to obtain any closed form solution, and this problem is highly favorable for solving by numerical methods. Hence, the matrix $[Y(\theta)]$ is obtained by using numerical integration, by use of the Runge-kutta integration method of forth order, with the starting value $[Y(0)]=[I]$ (unit matrix) which is given by taking $\theta=0$ in Eq. (18), and its solution depends only on the geometric and martial properties of the shell. For a plane passing through the central axis in a shell with structural symmetry, symmetrical and antisymmetrical profiles can be obtained, and consequently, only one-half of the shell circumferences are considered with the boundary conditions at the ends taken to be the symmetric or antisymmetric type of buckling deformations.

Therefore, the boundary conditions for symmetrical and antisymmetrical bucking deformations are $\tilde{V}=\tilde{\psi}_s=0,\ \tilde{S}_s=\tilde{N}_{sx}=0$ and

$$\tilde{U}=\tilde{W}=0,\ \tilde{N}_s=\tilde{M}_s=0, \text{Respectively} \tag{20}$$

4. BUCKLING LOADS AND BUCKLING MODES

The substitution of Eqs (20) into Eq. (18) results the buckling equations:

$$\begin{bmatrix} Y_{21} & Y_{23} & Y_{25} & Y_{27} \\ Y_{41} & Y_{43} & Y_{45} & Y_{47} \\ Y_{61} & Y_{63} & Y_{65} & Y_{67} \\ Y_{81} & Y_{83} & Y_{85} & Y_{87} \end{bmatrix}_{(\pi)} \begin{Bmatrix} \tilde{U} \\ \tilde{W} \\ \tilde{M}_s \\ \tilde{N}_s \end{Bmatrix}_{(0)} = 0 \qquad \text{For symmetrical modes,} \tag{21}$$

$$\begin{bmatrix} Y_{12} & Y_{14} & Y_{16} & Y_{18} \\ Y_{32} & Y_{34} & Y_{36} & Y_{38} \\ Y_{52} & Y_{45} & Y_{56} & Y_{58} \\ Y_{72} & Y_{74} & Y_{76} & Y_{78} \end{bmatrix}_{(\pi)} \begin{Bmatrix} \tilde{V} \\ \tilde{\psi}_s \\ \tilde{S}_s \\ \tilde{N}_{sx} \end{Bmatrix}_{(0)} = 0 \qquad \text{For antisymmetrical modes} \tag{22}$$

The matrices $[Y(\pi)]$ depend on the buckling load factor $\bar{p}$ and the circumferential angle θ. Equations (21) and (22) give a set of linear homogenous equations with unknown coefficients $\{\tilde{U},\tilde{W},\tilde{M}_s,\tilde{N}_s\}^T_{(0)}$ and $\{\tilde{V},\tilde{\psi}_s,\tilde{S}_s,\tilde{N}_{sx}\}^T_{(0)}$, respectively, at $\theta=0$. For the existence of a nontrivial solution of these coefficients, the determinant of the coefficient matrix should be vanished. The standard procedures cannot be employed for obtaining the eigenvalues of the load factor. The nontrivial solution is found by searching the values $\bar{p}$ which make the determinant zero by using Lagrange interpolation procedure. The critical buckling load of the shell will be the smallest member of this set of values. The buckling deformations (*circumferential buckling displacements mode*) at any point of the cross-section of the shell, for each axial half mode *m* are determined by calculating the eigenvectors corresponding to the eigenvalues $\bar{p}$ by using Gaussian elimination procedure.

5. COMPUTED RESULTS AND DISCUSSION

A computer program based on the analysis described herein has been developed to study the buckling characteristics of the shell under consideration. The critical buckling loads and the corresponding buckling deformations of the shell are calculated numerically, and some of the results shown next are for cases that have not as yet been considered in the literature. Our study is divided into two parts in which the Poisson's ratio ν takes the value 0.3.

5.1. BUCKLING RESULTS

Consider the buckling of a three-lobed cross-section cylindrical shell with circumferential variable thickness under non-uniform axial loads $p(\theta)$. The study of shell buckling is determined by finding the load factor $\bar{p}$ which equals the eigenvalues of (Eqs. (21) and (22)) for each value of *m*, separately. To obtain the buckling loads $p_B\ (=\bar{p})$ we will search the set of all eigenvalues, and to obtain the critical buckling loads $p_C\ (<p_B)$, which corresponds to loss of stability of the

shell, we will search the lowest values of this set. The numerical results presented herein pertain to the buckling loads in the case of uniform and non-uniform loads for symmetric and antisymmetric type-modes.

The effect of variation in thickness on the buckling loads, Table 1 gives the fundamental buckling loads factor of a three-lobed cross-section cylindrical shell with radius ratio ζ =0.5 versus the axial half wave number m for the specific values of thickness ratio η , symmetric and antisymmetric type- modes . A-columns correspond to the applied combined compression and bending loads, while B-columns are the applied axial compression loads, only.

The results presented in this table show that the increase of the thickness ratio tends to increase the critical buckling load (*bold number*) for each value of *m*. These results confirm the fact that the effect of increasing the shell flexural rigidity becomes larger than that of increasing the shell mass when the thickness ratio increases. It is shown by this table that the values of fundamental buckling loads for symmetric and antisymmetric modes are very close to each other for the large mode number *m*, and the buckling loads for symmetric and antisymmetrical modes have the same critical loads. The effect of applied combined loads makes the shell has critical loads some 1.5~2.5 times lower than applied compression loads, so that the shell buckles more readily and will be less stable for the combined loads. The ratio of critical loads μ takes the values within the (1.9 ~ 2.6) range and takes the smallest value 1.9 for the modes of the shell of constant thickness whereas the biggest value 2.6 for the shell of variable thickness. The critical buckling loads p_C for symmetrical modes occurred with *m*=5, except for compression load and constant thickness occurs with *m*=4, but for antisymmetrical modes those occurred with $m = 5$, and all for $l = 5$. Table 2 gives the fundamental buckling loads factor for a circular cylindrical shell of variable thickness versus the axial half wave number under the specific loads. As was expected that the symmetric and antisymmetric type-modes gives the same values of buckling loads factor versus the thickness ratio. It is seen from this table, in the case of applied combined axial loads, the shell will buckle more easily with increasing of axial half wave number *m* because of increasing of *m* results in decreasing of $\overline{p}$, whereas for more values of *m* the shell is less stable. In the case of applied compression loads and constant thickness ($\eta = 1$), the critical buckling load occurred for *m*=1, and an increase of *m* results in an increase of load factor and the shell will buckle hardly for *m* >1. For *m* >10 the shell will be more stable because the values of buckling load factor increase slightly until reach their convergence values between (230~231). Whereas in the case of combined loads a very fast convergence is observed in the lowest critical load value for *m* ≥17, With an increase of thickness ratio η the buckling loads increase for uniform and non-uniform loads, and they are lower values for the shell when the combined loads applied. For η >1, the ratio of critical loads μ is bigger than 2.4.

5.2. BUCKLING DEFORMATIONS

When a structure subjected usually to compression undergoes visibly large displacements transverse to the load then it is said to buckle, and for small loads the buckle is elastic since

buckling displacements disappear when the loads is removed. Generally, the buckling displacements mode is located at the weakest generatrix of the shell where the unsteady axial compression $p(\theta)$ is a maximum, and the shell has less stiffness. Figures (2) and (3) show the fundamental circumferential buckling modes of a three-lobed cross-section cylindrical shell of variable thickness under axial loads and combined compression and bending loads corresponding to the critical and the buckling loads factor listed in Tables (1) and (2), symmetric and antisymmetric type-modes. The thick lines show the composition of the circumferential and transverse deflections on the shell surface while the dotted lines show the original shell shape before buckling case. The numbers in the parentheses are the axial half wave number corresponding to the critical or buckling loads. There are considerable differences between the modes of $\eta=1$ and $\eta>1$ for the symmetric and antisymmetric type of buckling deformations. For $\eta=1$, in the case of axial load, the buckling modes are distributed regularly over the shell surface, but for $\eta>1$, the majority of symmetrical and antisymmetrical buckling modes, the displacements at the thinner edge are larger than those at the thicker edge i.e. the buckling modes are localized near the weakest lines on the shell surface. For $\eta=1$, in the case of non-uniform load, the buckling modes are located at the weakest generatix of the shell, where the axial compression load is a maximum in the compressive zone. For $\eta>1$, in the case of combined loads, the modes of buckling load are concentrated near the weakest generatrix on the shell surface in the compressive zone, but the modes of critical load are located at the tensile zone, where the axial load is a minimum and the thickness is a maximum. This indicates the possibility of a static loss of stability for the shell at values of p_B less than the critical value p_C. It can be also opined from these figures that the buckling behavior for the symmetric pattern is qualitatively similar to those of antisymmetric mode. Also, it is seen that the mode shapes are similar in the sets of the buckling modes having the ratio η >2 for the applied specific loads. Figure 4 shows the circumferential buckling modes of a circular cylindrical shell of variable thickness with ($l=4$ and $h=0.2$) under the specific loads. It is seen from this figure that the buckling deformations for applied uniform compression loads are distributed regularly over the shell surface of constant thickness, see Figures (i) and (ii). These figures are in quite good agreement with Ref. 5. It can be also seen from this figure that the shell of applied combined loads buckles more easily than one of applied compression loads.

Figure 5 shows the variations in the critical buckling loads of a non-uniformly loaded shell of a three lobed cross section and the corresponding values of the half wave number for ($1 \le m \le 20$) versus the radius ration ζ, for the specific values of thickness ratio η. The axial half wave number of corresponding critical buckling loads is shown in this figure as (m). It is seen from this figure, for the symmetric and antisymmetric type-modes, an increase in the radius ratio ζ causes an increase in the critical loads, and when the foregoing ratio becomes unity the latter quantities take the same values and assumed to be for a circular cylindrical shell. It is observed that the critical loads increase with an increase in the thickness ratio η where the shell becomes more stiffness. Upon increasing the radius ratio, the critical buckling axial half wave number increases. The nominal axial half wave number corresponding to the critical buckling load may be in general depends on the radius of curvature at the lobed corners of the shell.

Tables:

TABLE 1

The fundamental buckling loads factor $\overline{p}$ for symmetric and antisymmetric modes of a loaded cylindrical shell Of three lobed cross section with variable thickness, ($\zeta = 0.5,\ l = 5,\ h = 0.01$)

	Symmetric Modes η									Antisymmetric Modes η								
	1			2			5			1			2			5		
m	A	B	μ	A	B	μ	A	B	μ	A	B	μ	A	B	μ	A	B	μ
1	52.772	97.410	1.8	94.396	199.27	2.1	253.45	556.14	2.2	61.492	121.64	1.9	107.08	227.01	2.1	279.19	662.074	2.3
2	20.362	38.112	1.8	36.576	78.952	2.1	105.17	251.36	2.4	24.881	48.076	1.9	45.828	95.903	2.1	137.61	314.962	2.3
3	14.977	29.409	1.9	26.613	57.363	2.1	75.369	179.78	2.4	15.916	31.321	1.9	28.718	60.935	2.1	85.536	199.787	2.3
4	**13.577**	**26.904**	1.9	23.919	**51.713**	2.1	67.031	160.50	2.4	13.554	**26.963**	1.9	24.023	51.785	2.1	68.921	164.199	2.3
5	13.687	27.057	1.9	**23.849**	52.084	2.1	**65.112**	**157.91**	**2.4**	**13.498**	27.053	2.0	**23.478**	**51.421**	2.1	**64.284**	**156.245**	2.4
6	14.753	29.483	1.9	25.281	56.064	2.2	66.251	163.42	2.4	14.603	29.459	2.0	24.853	55.355	2.2	64.676	160.203	2.5
7	16.546	33.448	2.0	27.695	62.532	2.2	69.137	173.47	2.5	16.435	33.397	2.0	27.325	61.943	2.2	67.536	170.173	2.5
8	18.869	38.604	2.0	30.790	70.865	2.3	73.146	186.36	2.5	18.798	38.519	2.0	30.505	70.419	2.3	71.779	183.436	2.5
9	21.628	44.623	2.0	34.404	80.689	2.3	77.980	201.93	2.5	21.594	44.662	2.0	34.198	80.371	2.3	76.912	198.927	2.5
10	24.773	51.703	2.0	38.443	91.770	2.3	83.489	217.80	2.6	24.763	51.737	2.0	38.305	91.553	2.3	82.705	216.058	2.6

TABLE 2

The fundamental buckling loads factor $\overline{p}$ for symmetric and antisymmetric Modes of a loaded cylindrical shell, ($\zeta = 1,\ l = 5,\ h = 0.01$)

	Symmetric & Antisymmetric Modes η								
	1			2			5		
m	A	B	μ	A	B	μ	A	B	μ
1	292.341	592.423	2.0	379.178	912.032	2.4	652.296	1764.88	2.7
2	275.907	626.538	2.2	332.602	877.220	2.6	482.997	1354.82	2.8
3	265.975	641.974	2.4	308.969	838.994	2.7	415.423	1182.45	2.8
4	259.281	627.514	2.4	293.684	810.150	2.7	377.489	1083.87	2.8
5	254.345	628.201	2.4	283.038	789.053	2.7	352.558	1018.14	2.8
6	250.495	636.662	2.5	275.312	773.985	2.8	334.703	970.683	2.9
7	247.374	635.404	2.5	269.351	762.205	2.8	321.142	934.445	2.9
8	244.775	631.887	2.5	264.497	752.331	2.8	310.392	905.609	2.9
9	242.568	628.565	2.5	260.406	743.802	2.8	301.584	881.919	2.9
10	240.659	622.220	2.5	256.895	736.370	2.8	294.175	861.956	2.9

FIGURES:

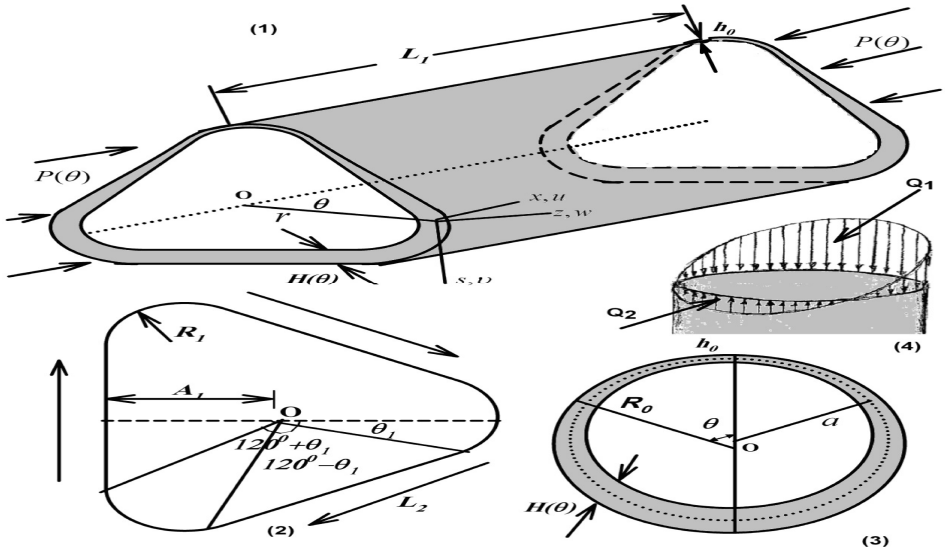

Fig: 1 coordinate system and geometry of a variable axial loaded cylindrical shell of three Lobed cross section with circumferential variable thickness

.

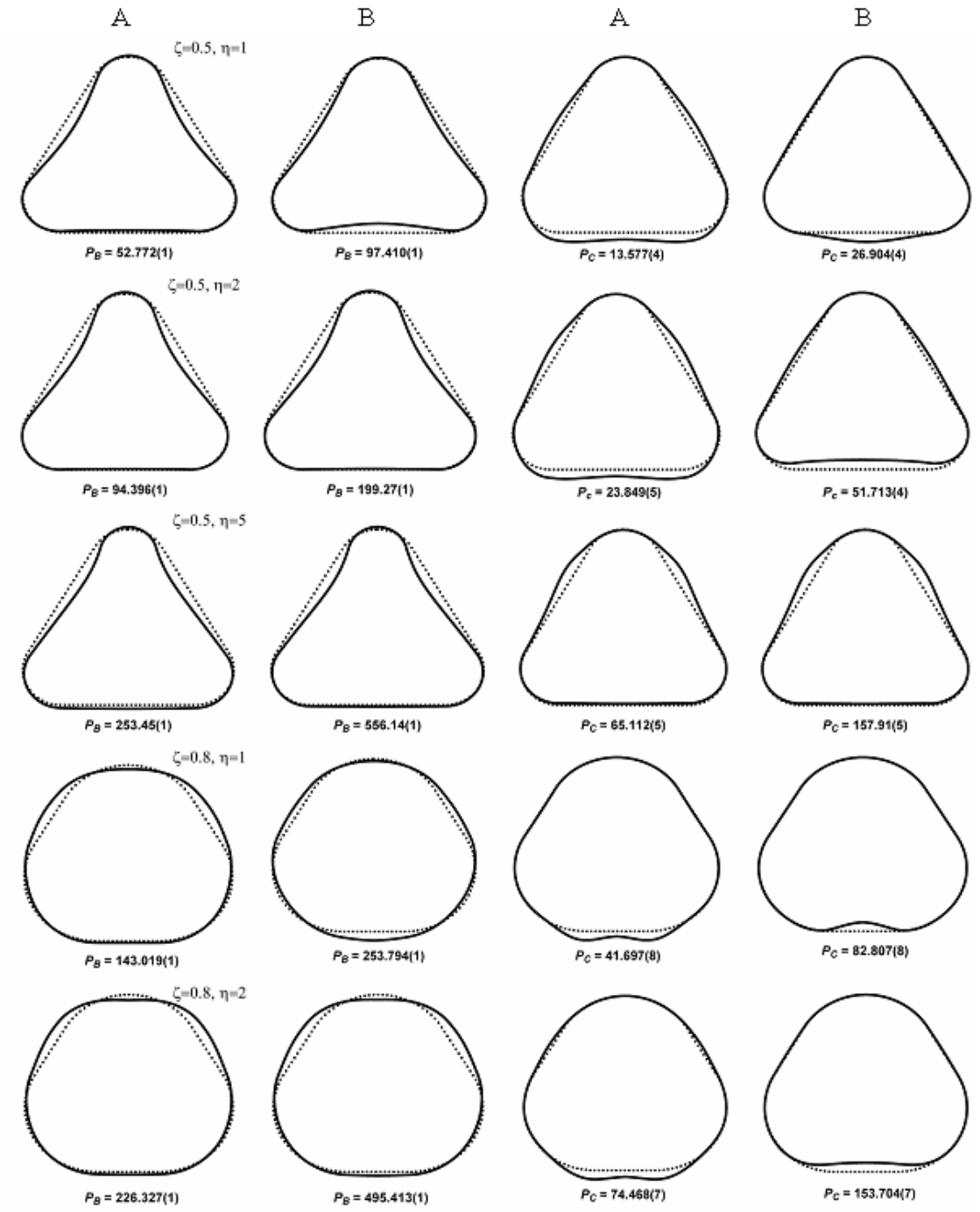

Fig: 2 the symmetric buckling deformations of a cylindrical shell of three lobed cross section With variable thickness $\{ l = 5, h = 0.01 \}$

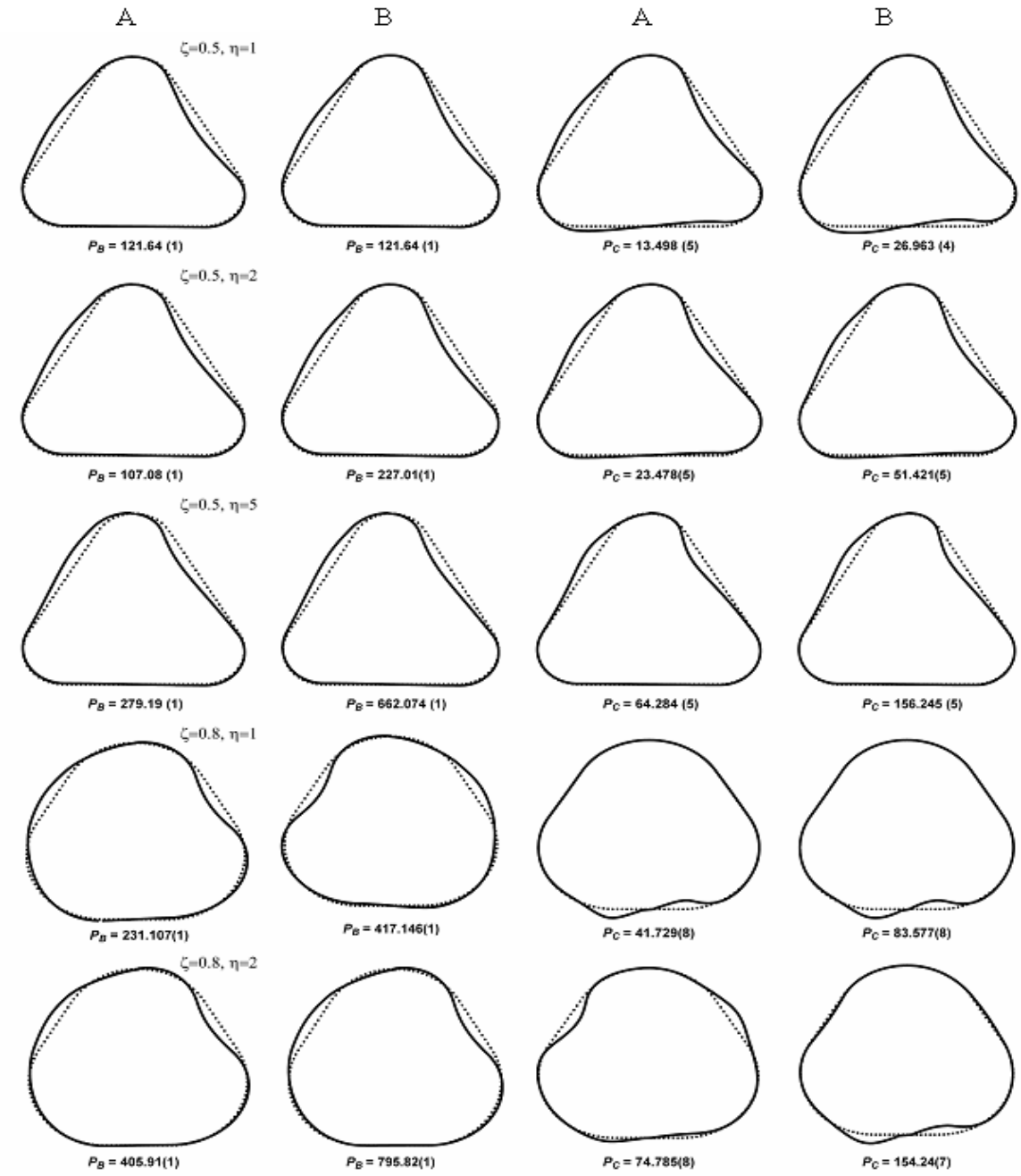

Fig: 3. the antisymmetric buckling deformations of a cylindrical shell of three lobed cross Section with variable thickness $\{ l = 5, h = 0.01 \}$

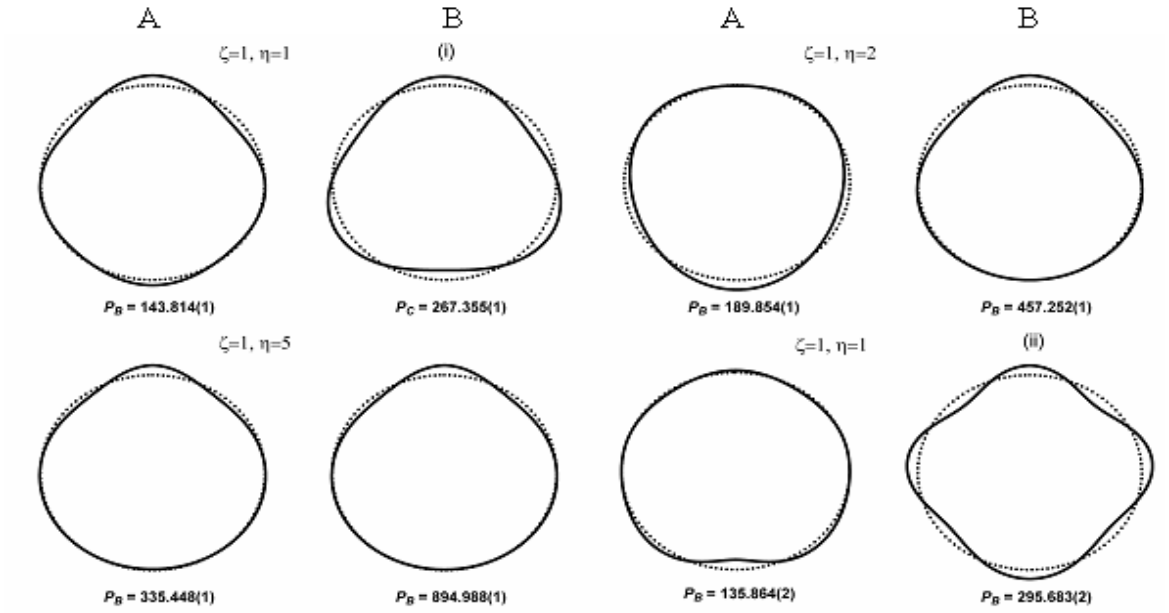

FIG: 4 THE CIRCUMFERENTIAL BUCKLING MODES OF A CIRCULAR CYLINDRICAL SHELL WITH VARIABLE THICKNESS.

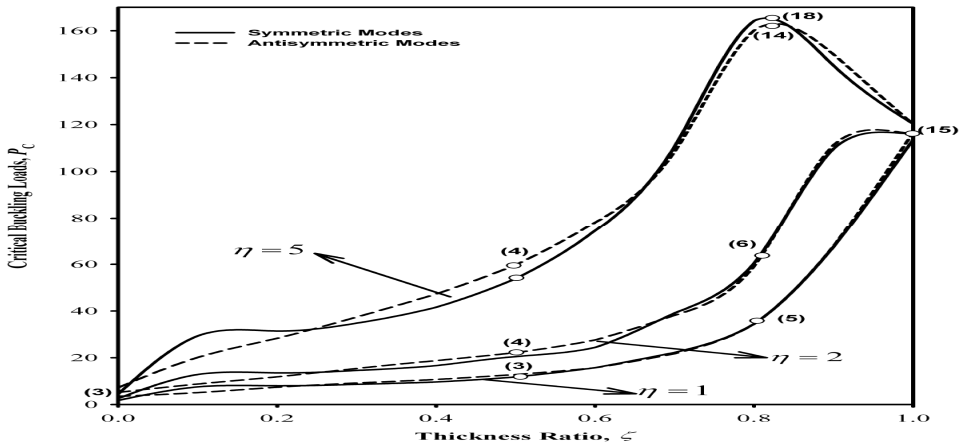

FIG: 5 CRITICAL BUCKLING LOADS VERSUS THICKNESS RATIO OF A THREE-LOBED CROSS-SECTION CYLINDRICAL SHELL WITH VARIABLE THICKNESS, ($l = 4$, $h = 0.02$)

6. CONCLUSIONS

An approximate analysis for studying the elastic buckling characteristics of circumferentially non-uniformly axially loaded cylindrical shell of a three-lobed cross-section having circumferential varying thickness is presented. The computed results presented herein pertain to the buckling loads and the corresponding mode shapes of buckling displacements by using the transfer matrix approach. The method is based on thin-shell theory and applied to a shell of symmetric and antisymmetric type-mode, and the analytic solutions are formulated to overcome the mathematical difficulties associated with mode coupling caused by variable shell wall curvature and thickness. The fundamental buckling loads and corresponding buckling deformations have been presented, and the effects of the thickness ratio of the cross-section and the non-uniformity of applied load on the critical loads and buckling modes were examined. The study showed that the buckling strength for combined loads was lower than that under compression loads. The deformations corresponding buckling load are located at the compressive zone of a small thickness but, in contrast, the deformations corresponding critical load are located at the tensile zone of a large thickness, and this indicates the possibility of a static loss of stability for the shell at values of less than the critical value P_C. Generally, the symmetric and antisymmeric buckling deformations take place in the less stiffened zones of the shell surface where the lobes are located. However, for the applied specific loads, the critical buckling loads increase with either increasing radius ratio or increasing thickness ratio and become larger for a circular cylindrical shell.

REFERENCES

[1] Seide P, Weigarten VI. On the buckling of circular cylindrical shells under pure bendin J Appl&Mech ASME Mar 1961: 112-16.

[2] Gerard G. Compressive stability of orthotropic cylinders J Aerospace Sci 1962; 29: 1171- 79

[3] Hoff JN, Soong CT. Buckling of circular cylindrical shells in axial compression Internet J Mech Sci 1965; 7: 489-520

[4] Stavsky Y, Friedland S. Stability of heterogeneous orthotropic cylindrical shells in axial Compression.Isr J Technol 1969; 7: 111-19

[5] Yamada G, Irie T, Tsushima M. Vibration and stability of orthotropic circular cylindrical shells subjected to axial load. J Acoust Soc Am 1984; 75(3): 842-48.

[6] Sabag M, Stavsky Y, Greenberge JB.Buckling of edge-damaged cylindrical composite Shells. J Appl Mech 1989; 56 (1): 121-26.

[7] Koiter I, Elishakoff Y, Starnes J. Buckling of an axially compressed cylindrical shell of Variable thickness Internet J Solids Structures 1994; 31: 797-805

[8] Teng JG. Buckling of thin shells, recent advantages and trends Applied Mechanics Review 1996; 17 (1): 73-83.

[9] Greenberg JB, Stavsky Y. Vibrations and buckling of composite orthotropic cylindrical Shells with nonuniform axial loads. Composites B 29B 1998: 695- 702

[10] Love AE. "A Treatise on the mathematical theory of elasticity", 1944 (Dover Publications, New York)

[11] Flügge W. "Stresses in shells. Springer", 1973 (Berlin)

[12] Tovstik PE. "Stability of thin shells", 1995 (Nauka, Moscow)

[13] Flügge W. Die stabilitat der kreiszylinderschale. Ingenieur Archiv 1932; 3: 463-506

[14] Bijlaard PP, Gallagher RH. Elastic instability of a cylindrical shell under arbitrary Circumferential variation of axial stresses.J Aerospace Sci 1959; 19(11): 854-858.

[15] Greenberg JB, Stavsky Y. Buckling of composite orthotropic cylindrical shells under Non-inform axial loads Composite Structures 1995; 30: 399-406

[16] Greenberg JB, Stavsky Y. Vibrations and buckling of composite orthotropic cylindrical shells with no uniform axial loads. Composite Part B 29B 1998: 695-703

[17] Avdoshka IV, Mikhasev GI. Wave packets in a thin cylindrical shell under a non-uniform axial load J Appl Maths&Mechs 2001; 65(2): 301- 9.

[18] Song C. Buckling of un-stiffened cylindrical shell under non-uniform axial compressive Stress. Journal of Zhejiang university Science 2002; 3(5): 520- 31.

[19] Abdullah H, Erdem H. The stability of non-homogenous elastic cylindrical thin shells with variable thickness under a dynamic external pressure Turkish J Eng Env Sci 2002; 26**:**155-64

[20] Eliseeva LS, Filippov SB. Buckling and vibrations of cylindrical shell of variable thickness with slanted edge. Vestnik Sankt-Peterskogo Universiteta 2003; 3**:** 84-91

[21] Filippov SB, Ivanov D, Naumova NV.Free vibrations and buckling of a thin cylindrical shell of variable thickness with curve linear edge. Technische Mechanic 2005; 25(1):1-8.

[22] Duan WH, Koh CG. Axisymmetric transverse vibrations of circular cylindrical shells with variable thickness.J Sound Vib 2008; 317: 1035-41.

[23] SambandamCT, Patel BP, Gupta SS, Munot CS, Granapathi M. Buckling characteristics of Cross-ply elliptical cylinders under axial compression Composite Structures 2003; 62: 7-17.

[24] Silvestre N. Buckling behaviour of elliptical cylindrical shells and tubes under compression Internet J Solids Structures 2008; 45: 4427-47.

[25] Khalifa M, Kobayashi Y, Yamada G. Vibration of non-circular cylindrical shells subjected to an axial load. Conference of JSME-D$D'98 1998: University of Hokkaido, Sapporo, Japan.

[26] Khalifa M. Buckling analysis of non-uniform cylindrical shells of a four lobed cross section under uniform axial compressions.ZAMM Z Angew Math Mech 2010; 90: 954-65

[27] Khalifa M. Vibration and buckling approximation of an axially loaded cylindrical shell with a three lobed cross section having varying thickness. Applied Mathematics 2011; 2 (3): 329-42.

[28] Tesar A, Fillo L. “Transfer matrix method”, 1988 (Dordrecht, Kluwer Academic).

[29] Goldenveizer AL. “Theory of thin shells”, 1961 (Pergamon Press, New York)

[30] Novozhilov VV. “The Theory of thin elastic shells”, 1964 (P. Noordhoff Ltd, Groningen, the Netherlands).

[31] Uhrig R. “Elastostatikund elastokinetikin matrizenschreibweise”, 1973 (Springer, Berlin)